

•Research article•

## Bufotenine and its derivatives: synthesis, analgesic effects identification and computational target prediction

ZHAO Chao, CHEN Min, SUN Shan-Liang, WANG Jiao-Jiao, ZHONG Yue, CHEN Huan-Huan, LI He-Min, XU Han, LI Nian-Guang\*, MA Hong-Yue\*, WANG Xiao-Long\*

National and Local Collaborative Engineering Center of Chinese Medicinal Resources Industrialization and Formulae Innovative Medicine, Jiangsu Collaborative Innovation Center of Chinese Medicinal Resources Industrialization, Jiangsu Key Laboratory for High Technology Research of TCM Formulae, Nanjing University of Chinese Medicine, Nanjing 210023, China

Available online 20 Jun., 2021

**[ABSTRACT]** Natural product bufotenine (**5**) which could be isolated from *Venenum Bufonis*, has been widely used as a tool in central nervous system (CNS) studies. We present here its quaternary ammonium salt (**6**) which was synthesized with high yields using 5-benzoyloxyindole as raw materials, and we firstly discover its analgesic effects *in vivo*. The analgesic evaluation showed that compounds **5** and **6** had stronger effects on the behavior of formalin induced pain in mice. Moreover, the combination of compound **6** and morphine has a synergistic effect. We intended to explain the molecular mechanism of this effect. Therefore, 36 analgesic-related targets (including 15 G protein-coupled receptors, 6 enzymes, 13 ion channels, and 2 others) were systemically evaluated using reverse docking. The results indicate that bufotenine and its derivatives are closely related to acetyl cholinesterase (AChE) or  $\alpha_4\beta_2$  nicotinic acetylcholine receptor (nAChR). This study provides practitioners a new insight of analgesic effects.

**[KEY WORDS]** Bufotenine; Analgesic; Reverse docking; Target prediction; Binding mode

**[CLC Number]** R284.2, R965 **[Document code]** A **[Article ID]** 2095-6975(2021)06-0454-10

### Introduction

Pain refers to unpleasant feelings or emotional experiences caused by tissue damage or potential damage. Severe pain not only brings anxiety to patients, but also causes physical dysfunction and even induces shock<sup>[1]</sup>. Meanwhile, pain can induce an early-warning physiological protective system, which is essential to detect and minimize the contact with damaging or noxious stimuli<sup>[2]</sup>. The causes of pain include cancer, inflammation or tissue injury, as well as lesions of the nervous system<sup>[3]</sup>. Currently, available drugs only achieve partial analgesia, and with problems such as poor efficacy and serious side effects<sup>[4]</sup>. Although the opioid analgesics and nonsteroidal anti-inflammatory drugs (NSAIDs) are currently used to treat pain, such as morphine, fentanyl, and as-

pirin. However, their clinical application is limited by some factors including analgesic tolerance, limited efficacy with slow improvement in clinical response and ‘heavy’ side effects or excessive costs<sup>[5]</sup>. Some of analgesics commonly in use were initially developed for the treatment of other diseases, which has poor selectivity. Due to this, these analgesics may reduce the compliance to the pharmacological therapy and resulted in the failure of pain treatment<sup>[6]</sup>. Therefore, there is a dire need for the development of novel analgesic drugs, with improved pharmaceutical profiles and reduced side effects, is still of great significance.

Small molecule compounds derived from natural products are receiving more and more attention in recent years. *Venenum Bufonis* (VB), which was isolated from the dried secretions of the skin and posteriority glands of *Bufo bufo gargarizans* Cantor and *Bufo melanostictus* Schneider, exhibited extensive biological activities including e.g. cardiotonic, diuretic, anti-tumor, local anesthesia, detoxify and analgesia<sup>[7]</sup>. The active ingredients of VB can be divided into liposoluble and water soluble components. Liposoluble components are mainly bufenolides, including bufalin (**1**), resibufogenin (**2**) and cinobufotalin (**3**), while water soluble ingredients principally refer to indole alkaloids such as serotonin (**4**) and bufotenine (**5**) (Fig. 1)<sup>[8]</sup>. Bufotenine, a trypt-

**[Received on]** 23-Nov.-2020

**[Research funding]** This work was supported by National Natural Science Foundation of China (No. 81973171), Postgraduate Research & Practice Innovation Program of Jiangsu Province (Nos. KYCX20\_1561 and SJCX20\_0533).

**[\*Corresponding author]** Tel/Fax: 86-25-85811916, E-mail: linian-guang@njucm.edu.cn (LI Nian-Guang); E-mail: hongyuema@njucm.edu.cn (MA Hong-Yue); E-mail: gregwang@njucm.edu.cn (WANG Xiao-Long)

These authors have no conflict of interest to declare.

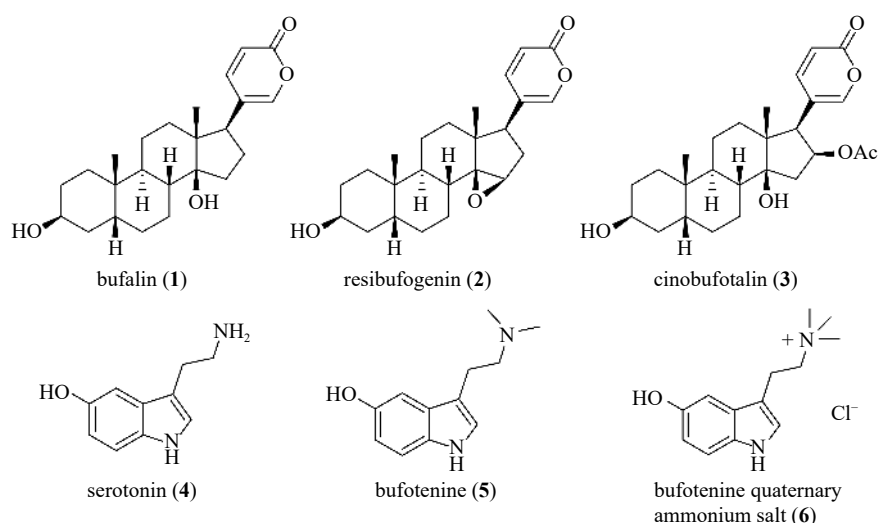


**Fig. 1 Structures of representative ingredients in VB (1–5) and compound 6**

amine alkaloid resulting from the methylation of serotonin (4), which is a signaling molecule that can alleviate the severity of analgesic and its syndrome. Moreover, serotonin has been demonstrated, in both animal and human studies, that serotonergic signaling elements can have a major impact on inflammation development and severity [9]. Therefore, bufotenine might play a vital role in analgesic activity of VB. In order to investigate this, we synthesized bufotenine (5) alongside with its quaternary ammonium salt (6) (Fig. 1). The analgesic activities of the two compounds were evaluated on the behavior of formalin induced pain in mice. The analgesic evaluation showed that compound 5 and compound 6 had strong effects on the behavior of formalin induced pain in mice. Moreover, the combination of compound 6 and morphine has a synergistic analgesic effect.

We have discovered a natural product molecules bufotenine and its salt, which show obvious analgesic effects. In order to discover their mechanism, computational technologies were used to predict potential receptors. Literatures study indicated several targets relating to analgesic effects [10], and in order to further investigate the molecular mechanism of this effect, we are mainly focus on the 36 targets (Table 1) which with released crystal structures. According to their physiological functions, these targets are can be classified into i) G protein-coupled receptors (GPCRs), e.g. serotonin 5-HT<sub>1B</sub>, 5-HT<sub>2A</sub>, 5-HT<sub>2B</sub>, 5-HT<sub>2C</sub> receptors, opioid  $\delta$ ,  $\kappa$ ,  $\mu$ , and NOP receptors, cannabinoid 1 receptor CB<sub>1</sub>, neurokinin-1 receptor NK<sub>1</sub>, metabotropic glutamate receptor 5 mGLUR<sub>5</sub>, adenosine receptors A<sub>1</sub> and A<sub>2A</sub>, neurotensin-1 receptor NTS<sub>1</sub>, angiotensin type 2 receptor AT<sub>2</sub>; ii) enzyme, e.g. cyclooxygenase 1 COX-1, acetylcholinesterase AChE, nitric oxide synthase NOS, sepiapterin reductase SPR, microsomal prostaglandin E synthase-1 mPGES1 and soluble epoxide hydrolase SEH; iii) ion channel e.g. voltage-gated sodium channels (NaV1.7), TWIK-Related K<sup>+</sup> Channel 1 TREK-1 (K2P, KV7 and KV2), acidsensing ion channels ASICs, N-methyl-

D-aspartic acid NMDA2A, transient receptor potential vanilloid TRPV1 and TRPA1,  $\alpha 7/\alpha 4\beta 2$  nicotinic acetylcholine receptors  $\alpha 7/\alpha 4\beta 2$  nAChR, P2X3 ATP receptors and  $\gamma$ -aminobutyric acid GABA; and i.v.) others, e.g. tumor necrosis factor- $\alpha$  TNF- $\alpha$  and tropomyosin receptor kinase A TrkA. All these analgesic effects-related targets are used for computational target prediction.

Reverse docking, a computational method which involves docking a ligand in potential binding sites of a set of targets, has been proved to be a powerful tool for drug repositioning [11]. In contrast with traditional molecular docking, reverse docking ranks target proteins for a given ligand rather than ligands for a given target protein. Base on the list of ranked target proteins, the relevance of a given ligand for potential target(s) can be estimated. Therefore, the reverse docking method is useful for searching potential targets of drugs already approved [12] or of natural products [13] whose mechanism are not yet known. Several studies have been performed to predict targets successfully. Here we performed reverse dockings to predict potential targets of bufotenine (5) and its derivatives (6), that could produce analgesic effect. In addition, all the docking poses were subsequently post-processed by protein-ligand binding free energy simulations (molecular mechanics-generalized4 Bornsurface area, MMGBSA). In MMGBSA, the free binding energy simulation combined gas phase energy (MM), electrostatic solvation energy (GB), as well as nonelectrostatic contribution to solvation energy (SA). The MMGBSA methods have become widely adopted in estimating protein-ligand binding affinities due to their efficiency and high correlation with experiment [14]. Based on computational prediction (e.g. reverse docking and binding free energy prediction), experimental validation was followed and acetylcholinesterase AChE was finally identified as the target. Moreover, binding modes hypotheses between compound 6 and AChE is presented.

Table 1

| Class | Target             | PDB <sup>a</sup> | Glide <sup>b</sup> | MMGBSA | Class | Target             | PDB    | Glide  | MMGBSA | Class       | Target              | PDB    | Glide  | MMGBSA |
|-------|--------------------|------------------|--------------------|--------|-------|--------------------|--------|--------|--------|-------------|---------------------|--------|--------|--------|
|       | A <sub>1</sub>     | 5N2S             | -6.06              | -40.07 |       | 5-HT <sub>1B</sub> | 5V54   | -2.19  | -47.35 |             | SPR                 | 6I6V_2 | -5.07  | -43.02 |
|       | A <sub>1</sub>     | 5UEN             | -5.40              | -36.95 |       | 5-HT <sub>1B</sub> | 4IAQ   | -5.28  | -39.66 |             | AchE                | 6TTO   | -11.79 | -83.63 |
|       | A <sub>2A</sub>    | 3UZA             | -6.48              | -36.07 |       | 5-HT <sub>1B</sub> | 4IAR   | -6.76  | -38.09 | Enzyme      | AchE                | 1ZGB   | -10.51 | -44.83 |
|       | A <sub>2A</sub>    | 5IU4             | -7.15              | -47.32 |       | 5-HT <sub>1B</sub> | 6G79   | -5.30  | -37.65 |             | AchE                | 6XYU   | -12.55 | -40.83 |
|       | A <sub>2A</sub>    | 5IU7             | -7.42              | -25.94 |       | 5-HT <sub>2A</sub> | 6A93   | -6.07  | -43.37 |             | AchE                | 2ACK   | -4.63  | -28.97 |
|       | A <sub>2A</sub>    | 5K7K             | -6.52              | -0.23  |       | 5-HT <sub>2A</sub> | 6A94   | -4.79  | -35.26 |             |                     |        |        |        |
|       | A <sub>2A</sub>    | 5OLG             | -6.92              | -47.38 |       | 5-HT <sub>2B</sub> | 5TUD   | -10.17 | -43.92 |             | ASIC1               | 2QTS   | -2.62  | -28.42 |
|       | AT <sub>2</sub>    | 5UNF             | -5.15              | -33.94 |       | 5-HT <sub>2B</sub> | 6DS0   | -5.98  | -40.54 |             | GABA3               | 4TK3   | -3.92  | -33.45 |
|       | AT <sub>2</sub>    | 5UNG             | -5.57              | -28.03 | GPCR  | 5-HT <sub>2B</sub> | 6DRZ   | -9.15  | -39.07 |             | GABA1               | 5OSA   | -2.71  | -27.80 |
|       | AT <sub>2</sub>    | 5UNH             | -4.80              | -34.74 |       | 5-HT <sub>2B</sub> | 4NC3   | -8.79  | -38.91 |             | TREK2               | 4XDK   | -4.59  | -36.77 |
|       | CB <sub>1</sub>    | 5TGZ             | -5.96              | -33.17 |       | 5-HT <sub>2B</sub> | 4IB4   | -5.69  | -37.28 |             | TREK2               | 4XDL   | -4.54  | -38.58 |
|       | CB <sub>1</sub>    | 5U09             | -5.59              | -47.54 |       | 5-HT <sub>2B</sub> | 6DRX   | -6.66  | -34.96 |             | TREK2               | 6CQ8   | -3.89  | -34.90 |
|       | CB <sub>1</sub>    | 5XR8             | -5.97              | -48.00 |       | 5-HT <sub>2B</sub> | 5TVN   | -7.57  | -33.48 |             | TREK1               | 6CQ9   | -5.53  | -30.60 |
|       | CB <sub>1</sub>    | 5XRA             | -5.97              | -51.76 |       | 5-HT <sub>2B</sub> | 6DRY   | -6.96  | -31.49 |             | TREK1               | 6V37   | -4.43  | -31.88 |
|       | CB <sub>1</sub>    | 6KPG             | -6.02              | -44.43 |       | 5-HT <sub>2C</sub> | 6BQH   | -5.52  | -48.16 |             | TREK2               | 3LNM   | -6.80  | -32.78 |
|       | CB <sub>1</sub>    | 6N4B             | -9.55              | -41.81 |       | 5-HT <sub>2C</sub> | 6BQG   | -5.87  | -42.94 |             | NaV1.7              | 5EKO   | -4.73  | -42.39 |
|       | mGluR <sub>5</sub> | 4O09             | -0.52              | -37.15 |       | GLP <sub>1</sub>   | 3IOL   | -4.50  | -23.75 |             | NaV1.7              | 5KOI   | -2.85  | -25.53 |
|       | mGluR <sub>5</sub> | 5CGC             | -2.96              | -40.16 |       | COX1               | 3KK6   | -7.90  | -49.28 |             | NaV1.7              | 6J8G   | -4.65  | -22.50 |
|       | mGluR <sub>5</sub> | 5CGD             | -7.72              | -36.93 |       | COX1               | 3N8Y   | -2.66  | -32.79 |             | NaV1.7              | 6J8H   | -4.73  | -18.39 |
|       | NK <sub>1</sub>    | 6E59             | -6.69              | -40.73 |       | COX1               | 5WBE   | -6.35  | -48.51 |             | NaV1.7              | 6J8I   | -3.66  | -18.49 |
|       | NK <sub>1</sub>    | 6HLL             | -6.90              | -38.25 |       | mPGES1             | 4WAB   | -2.07  | -23.33 |             | NaV1.7              | 6J8J   | -6.11  | -20.64 |
| GPCR  | NK <sub>1</sub>    | 6HLO             | -5.00              | -37.29 |       | mPGES1             | 4YL3   | -1.32  | -19.25 |             | NMDA2A              | 5VII   | -3.24  | -32.01 |
|       | NK <sub>1</sub>    | 6HLP             | -6.03              | -31.28 |       | mPGES1             | 5BQG   | -2.63  | -24.77 | Ion Channel | GluA2               | 6Q54   | -2.21  | 41.95  |
|       | NK <sub>1</sub>    | 6J21             | -6.01              | -32.83 |       | mPGES1             | 5K2D   | -6.91  | -35.30 |             | P2X <sub>3</sub>    | 5SVK   | -2.73  | -20.39 |
|       | δ                  | 4EJ4             | -3.63              | -33.52 |       | mPGES1             | 5T37   | -2.41  | -26.57 |             | P2X <sub>3</sub>    | 5YVE   | -4.64  | -32.51 |
|       | δ                  | 4N6H             | -3.85              | -33.78 |       | NOS                | 1M7Z   | -4.62  | -34.28 |             | P2X <sub>3</sub>    | 6AH4   | -2.89  | -25.33 |
|       | δ                  | 4RWA             | -5.99              | -33.08 |       | NOS                | 2FBZ   | -2.88  | -30.29 |             | TRPA <sub>1</sub>   | 6PQO   | -5.12  | -36.60 |
|       | δ                  | 4RWD             | -2.57              | -27.68 |       | NOS                | 4CU1   | -4.16  | 6.82   |             | TRPA <sub>1</sub>   | 6V9V   | -5.05  | -34.55 |
|       | δ                  | 6PT2             | -4.01              | -35.91 |       | NOS                | 5G6B_1 | -6.33  | 5.48   |             | TRPA <sub>1</sub>   | 2PNN   | -3.46  | -32.00 |
|       | δ                  | 6PT3             | -3.45              | -38.53 |       | NOS                | 5G6B_2 | -4.53  | -27.33 |             | TRPV <sub>1</sub>   | 5IRX   | -6.11  | -38.08 |
|       | κ                  | 4DJH             | -7.48              | -29.96 |       | NOS                | 5VV6_1 | -4.06  | -21.93 | Enzyme      | Na <sub>v</sub> PaS | 6A95   | -5.13  | -38.84 |
|       | κ                  | 6B73             | -5.88              | -36.79 |       | NOS                | 5VV6_2 | -5.96  | -2.26  |             | AchBP               | 3ZDG   | -7.40  | -36.84 |
|       | κ                  | 6VI4             | -5.90              | -38.38 |       | SEH                | 3ANS   | -5.21  | -51.60 |             | AchBP               | 4AFH   | -11.17 | -48.41 |
|       | μ                  | 4DKL             | -8.46              | -27.03 |       | SEH                | 3WKB   | -4.82  | -37.27 |             | AchBP               | 4B5D   | -12.18 | -37.29 |
|       | μ                  | 5C1M             | -2.44              | -40.25 |       | SEH                | 4OD0   | -9.51  | -35.14 |             | AchA7               | 3SIO   | -10.07 | -39.24 |
|       | NOP                | 4EA3             | -5.65              | -35.66 |       | SEH                | 5MWA   | -6.27  | -31.48 |             | AchA7               | 5AFN-1 | -2.75  | -44.04 |
|       | NOP                | 5DHH             | -4.61              | -35.90 |       | SPR                | 4HWK_1 | -6.17  | -37.34 |             | AchA7               | 5AFN-2 | -4.68  | -32.84 |
|       | NTS <sub>1</sub>   | 4BV0             | -5.31              | -36.42 |       | SPR                | 4HWK_2 | -5.90  | -38.26 |             | AchA7               | 5J5G   | -3.81  | -34.63 |
|       | NTS <sub>1</sub>   | 4GRV             | -6.90              | -35.54 |       | SPR                | 4XWY_1 | -3.10  | -30.11 |             | AchA7               | 5OUH   | -5.13  | -33.46 |
|       | NTS <sub>1</sub>   | 4XEE             | -8.09              | -38.30 |       | SPR                | 4XWY_2 | -5.14  | -47.01 |             |                     |        |        |        |
|       | NTS <sub>1</sub>   | 4XES             | -8.15              | -42.62 |       | SPR                | 4Z3K_1 | -5.47  | -37.39 |             | TNF-α               | 1fT4   | -1.98  | -20.16 |
|       | NTS <sub>1</sub>   | 3ZEV             | -8.81              | -35.20 |       | SPR                | 4Z3K_2 | -4.91  | -36.23 | Others      | TrkA                | 6IQN   | -7.13  | -40.17 |
|       | NTS <sub>1</sub>   | 4BUO             | -9.71              | -35.76 |       | SPR                | 6I6V_1 | -6.04  | -40.40 |             | TrkA                | 6NSS   | -4.14  | -35.51 |

## Results and Discussion

### Chemistry

Bufotenine (**5**) and bufotenine quaternary ammonium salt (**6**) were synthesized in high yields using 5-benzyloxyindole as raw materials as shown in Scheme 1. 5-Benzyloxyindole (**7**) was acylated with oxalyl chloride to give compound **8** with a crude yield of 94%, and then reacted compound **8** with dimethylamine hydrochloride in an alkaline environment afforded compound **9** in 90% yield. Subsequently the benzyl protecting group was removed under the condition of 10% palladium on activated carbon with H<sub>2</sub>, and the important intermediate compound **10** was obtained in 92% yield. Taking into this account that both ketone-carbonyl groups must be converted to methylene, so we focused our attention to optimize the reduction conditions of compound **10** and LiAlH<sub>4</sub> to produce the target compound **5**. We chose anhydrous tetrahydrofuran as a reaction solvent, the molar ration of compound **10** : LiAlH<sub>4</sub> is 1 : 6, and finally compound **5** is obtained with a yield of 85%<sup>[15]</sup>. The target compound **6** in the form of a quaternary ammonium salt of compound **5** was obtained. Based on the synthesis of compound **5** by our research team, we selected a suitable reaction solvent—methanol and under dark conditions, then allowing compound **5** to react with excess methyl iodide to obtain a compound in the form of iodized salt. Considering the instability of the iodized salt, after the reaction is completely treated, silver chloride is added for substitution to obtain a stable structure of compound **6** with a yield of 90%.

### Analgesic evaluation

#### Behavior effects of formalin-induced pain model

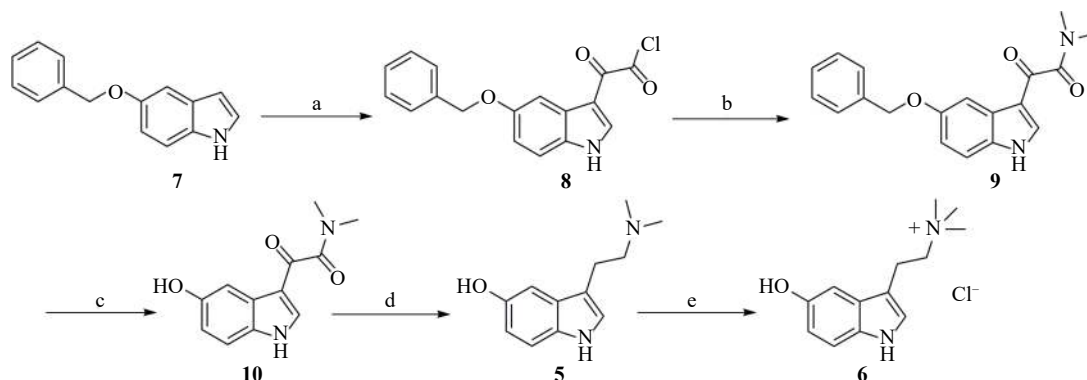
The painful reaction of formalin foot swelling manifests as a biphasic response, one phase (0–5 min; the first stage) belongs to the surrounding nociceptors that are directly stimulated by formalin, the second phase (15–45 min; The second stage) belongs to the central neuron sensitization process, with a relatively short resting period (5–10 min) during this period, also called analgesia incubation period. In this test, formalin's nociceptive behavior was quantified as the length of time of licking or biting injection foot within 45 min (di-

vided into 9 cycles of 5 min each). Behavior of licking/biting their paws was recorded and the lower time of the paw licking/biting indicated a better analgesic activity. Behavior results showed that all groups experienced a relatively short resting period after peripheral nociceptive pain caused by formalin in the 5–10 min phase. The intraperitoneal injection (i.p.) of compounds **5** (5, 15 mg·kg<sup>-1</sup>) and **6** (5, 15 mg·kg<sup>-1</sup>) groups exhibited apparent decreases in the licking/biting from the 10 min to the 45 min ( $P < 0.0001$  vs control,  $n = 12$ ). Moreover, we discovered that compound **6** has better inhibition effect than compound **5**, and compound **6** (15 mg·kg<sup>-1</sup>) has better inhibition effect than compound **6** (5 mg·kg<sup>-1</sup>) (Fig. 2). *Synergistic analgesic effect of co-administration of compound 6 with morphine*

In the test, we evaluated the analgesic effect and forms of compound **6** combined with morphine. With the treatment of morphine (0.25 mg·kg<sup>-1</sup>) group and compound **6** (5, 15 mg·kg<sup>-1</sup>) groups respectively, after 60 min of intraperitoneal administration (i.p.). The results showed that the compound **6** (5 mg·kg<sup>-1</sup>) group used alone could slightly extend the paw withdrawing thermal latency (PWTL) of mice hind foot on the hot plate, and the morphine (0.25 mg·kg<sup>-1</sup>) and the compound **6** (15 mg·kg<sup>-1</sup>) groups are apparently increased the first foot lift time ( $P < 0.05$  vs control,  $n = 12$ ). However, when the above doses of drugs were used in combination (morphine + compound **6**), the first foot lift time is remarkable enhanced ( $P < 0.0001$  vs control,  $n = 12$ ), the prolonged analgesic activity of mice obviously increased from 125.2% and 138.4% to 175.9% and 195.6%, the groups produced a significant analgesic effect and shows that the combination of compound **6** and morphine has a synergistic effect. Unfortunately, after 90 min of administration, the synergistic analgesic effect of the combination group was apparently weakening, indicating that compound **6** may have the potential for short-acting analgesia (Fig. 3A and 3B).

#### Reverse docking for target prediction

To identify the analgesic mechanism of bufotenine and its derivatives, we performed reverse docking with a database of 127 crystal structures covering 36 analgesic-related



**Scheme 1** Reagents and conditions: (a) (COCl)<sub>2</sub>, Et<sub>2</sub>O, r.t., 30 min, 94%; (b) NH(CH<sub>3</sub>)<sub>2</sub>, NaOH(aq), Et<sub>2</sub>O, r.t., 45 min, 90%; (c) 10% Pd/C, H<sub>2</sub>, CH<sub>3</sub>OH, THF, r.t., 18 h, 92%; (d) LiAlH<sub>4</sub>, dry THF, 4 h, reflux, r.t., 10 h, 85%; (e) CH<sub>3</sub>I, CH<sub>3</sub>OH, r.t., 36 h; AgCl, CH<sub>3</sub>OH, 24 h, 90%

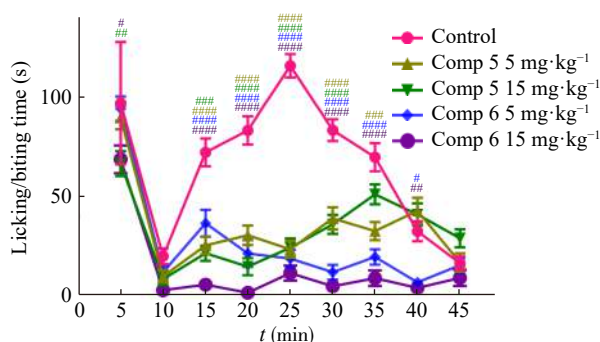


**Fig. 2** Effect of compounds **5** and **6** on analgesic parameters of ICR mice (a) Licking/biting time. (a) values represent as mean  $\pm$  SEM of twelve observations. #  $P < 0.05$ , ##  $P < 0.01$  ###  $P < 0.001$ , and ####  $P < 0.0001$  vs control. (Statistical significance was assessed by two-way ANOVA followed by Dunnett's  $t$  test)

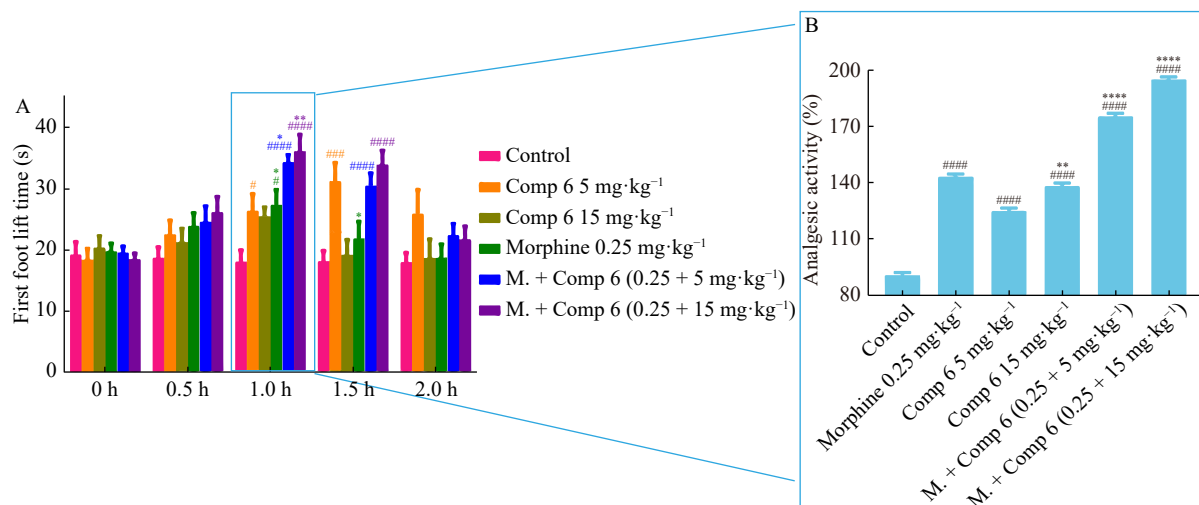
target proteins. In order to further model molecular recognition, both XP GlideScore and MMGBSA (molecular mechanics-generalized Born surface area, MMGBSA) are involved (Table 1). The docking score GlideScore<sup>[16]</sup> is an empirical scoring function which has many terms including force field and terms rewarding or penalizing interactions known to influence ligand binding. While the MMGBSA methods have become widely adopted in estimating protein-ligand binding affinities due to their efficiency and high correlation with experiment<sup>[14]</sup>. All the docking poses are subsequently post-processed by MMGBSA calculations. Based on the Glide Gscore and protein-ligand binding free energy MMGBSA scores, the poses with the lowest XP GlideScores were selected for further analysis.

Table 1 (in supporting information) shows the performance of 36 analgesic-related target proteins based on Glide

XP Scores and MMGBSA. Cutoffs for GlideScore and MMGBSA are set based on top 20% ranked structures, and  $-7.0$  and  $-40$  are indicated, respectively. Glide scorings gives 18.1% structures with GlideScore  $\leq -7.0$ , while 18.9% structures with MMGBSA scores  $\leq -40$ , and covering 13 and 15 receptors, respectively. However, 10 structures covering 8 receptors ( $A_{2A}$ ,  $CB_1$ ,  $NTS_1$ ,  $5-HT_{2B}$ ,  $5-HT_{2C}$ ,  $COX1$ ,  $AChE$ ,  $AChBP$  and  $TrkA$ ) simultaneously meet the cutoffs of both Glide Gscores and MMGBSA scores (Fig. 4A). Interestingly, it is obviously to find that both GlideScores and MMGBSA are enriched in acetylcholinesterase (AChE), of which 3 of 4 structures are out-performed. Moreover, the best Glide Gscore ( $-12.6$ ) and MMGBSA ( $-83.6$ ) are observed from AChE as well. Although enrichment of GlideGscore are observed in  $NTS_1$  and  $5-HT_{2B}$  receptors, and MMGBSA are likely to enrich in  $CB_1$  and  $5-HT_{(X)}$  receptors, it is hard for these targets to obtain both scores cutoffs as set. For example, MMGBSA indicate 5 of 6  $CB_1$  structures outperformed most of other targets. However, their GlideScores are much lower (most are around 6.0) than the set cutoff value. Similarly,  $NTS_1$  performed well (4 of 6 structures are lower than  $-8.0$ ) if ranked on GlideScore, while the profiles of MMGBSA are inferior.

Further increased the cutoffs (top 5%) of Glide XP score and MMGBSA score to  $-9.5$  and  $-48.0$  (Fig. 4B), 8 receptors are reserved including GPCRs  $5-HT_{2C}$ ,  $CB_1$  and  $NTS_1$ , enzyme SEH, AChE and  $COX1$ , and ion channel AChBP and AChA7 (Figs. 5 and S7-S11). Fig. 4B shows that nAChR (AChBP) and AChE meet the even more strict cutoffs of both Glide XP score and MMGBSA, indicating the most potential binding targets.

Interestingly, Khorana *et al.*<sup>[17]</sup> found that compound **4** performed 62% inhibition on AChE at concentration  $3.4 \times$



**Fig. 3** Synergistic analgesic effect of compound **6** combined with morphine: (A) represents the first foot lift time of synergistic analgesic effect of compound **6** combined with morphine by hot plate method, graph (B) respectively showing the analgesic activity in mice after 60 min drug intervention. Represented values are the mean  $\pm$  SEM of twelve observations. #  $P < 0.05$ , ##  $P < 0.01$  and ###  $P < 0.001$  vs control group; \*  $P < 0.05$ , \*\*  $P < 0.01$  and \*\*\*  $P < 0.001$  vs morphine group (Statistical significance was assessed by one-way ANOVA followed by Dunnett's  $t$  test)

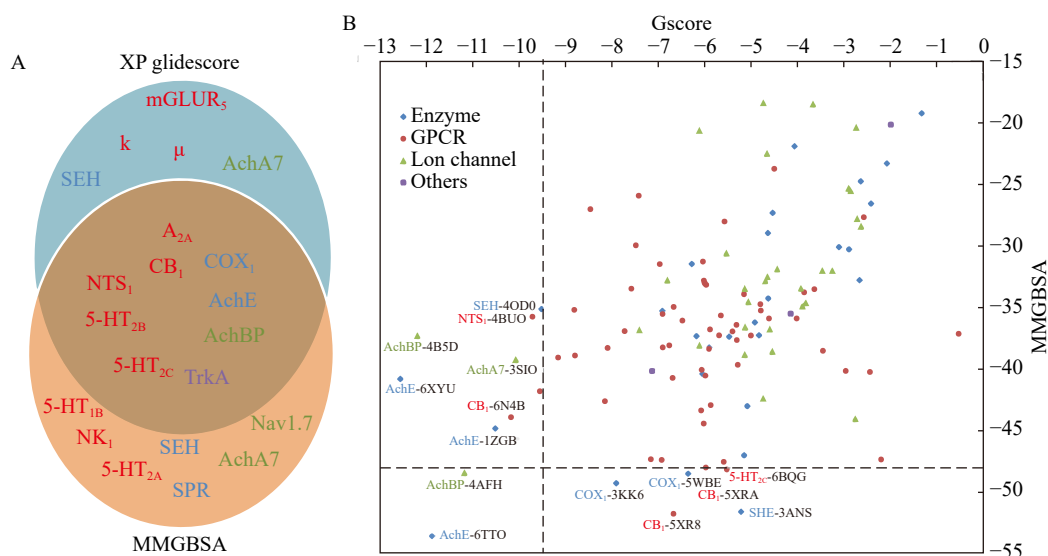


**Fig. 4** A) Venn diagrams based on Glide XP Score and MMGBSA lower than  $-7.0$  and  $-40$ , respectively. B) Scatterplot of Glide XP Gscore versus MMGBSA DG binding scores which is derived from Table 1. Targets are classified into enzyme, G protein-coupled receptor (GPCR), ion channel and others, and are shown in blue, red, green and orange, respectively. The cutoffs (dot lines) of the top 5% ranked Glide Gscore and MMGBSA are  $-9.5$  and  $-48.0$ , respectively

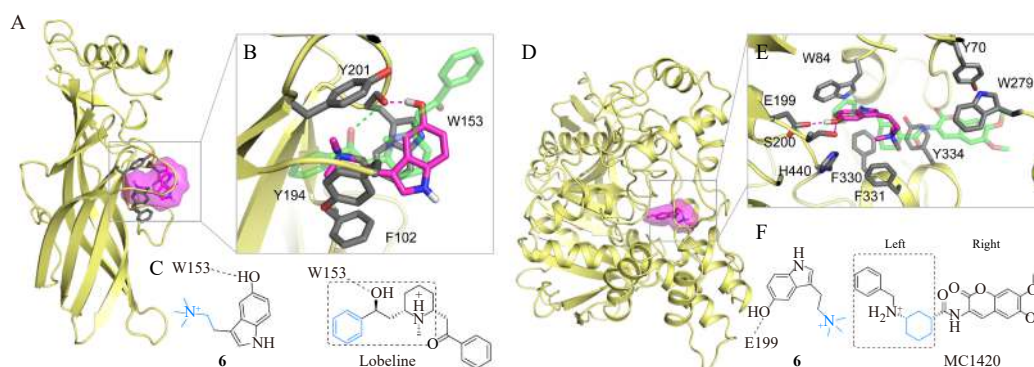


**Fig. 5** Overview of compound **6** (magenta stick and transparent surface) bound to AChBP (A, PDB: 4AFH, yellow cartoon) and AchE (D, PDB: 6TT0, yellow cartoon). B) and E) Detailed comparison of the binding modes of compound **6** (transparent magenta stick) and lobeline (green stick) in AChBP, as well as compound **6** (magenta stick) and MC1420 (transparent green stick) in AchE, and key residues are shown as gray sticks. C) and F) Chemical structure of compound **6**, lobeline, and MC-1420, polar interactions between ligands and specific residue are depicted in dotted lines. The sub-group of lobeline which is aligned with compound **6** is indicated in dotted box, and the groups targeting the hydrophobic area of AChBP are shown in blue

$10^{-4}$  mol·L<sup>-1</sup>, however IC<sub>50</sub> was not determined. While Queiroz *et al.* [18] determined compounds **5** with IC<sub>50</sub> of 11.4 μmol·L<sup>-1</sup> on AchE. The only difference between the two compounds is that **5** contains two methyl groups which may form hydrophobic interaction with receptor residues, and resulted in bioactivity on AchE. Detailed binding modes comparisons will be discussed in the following section.

#### Binding site characterization

##### $\alpha_4\beta_2$ nicotinic acetylcholine receptor (nAChR)

Compound **6** can well bound to the site of nAChR (AChBP) (Fig. 5A) where the co-crystallized ligand lobeline binds, and shows similar binding modes as lobeline (Figs. 5B and 5C). Both compound **6** and lobeline can form hydrogen bond with Trp153 through phenolic hydroxyl group and hydroxyl, respectively (Fig. 5B and 5C). One hydrophobic area

is observed in the interior of the pocket which is composed of several aromatic residues, e.g. Phe102, Trp153, Tyr194, and Tyr201. Further comparison indicates that both the trimethylammonium groups in compound **6** and the benzene ring of lobeline can target this hydrophobic sub-pocket (Fig. 5C) in AChBP.

##### Acetylcholinesterase (AChE)

Compound **6** is chemically different from MC1420, but can target the same binding site (Fig. 5D). Interestingly, crystal structure shows no polar interaction between AchE residues and MC1420, while the phenolic hydroxyl group of **6** forms hydrogen bond interaction with Glu199. Obviously, F330, F331, Y334 and H440 in AchE form a hydrophobic pocket and establish hydrophobic contacts with cyclohexane of MC1420. Binding mode indicates the trimethylammonium

group of **6** are also located in the hydrophobic area. Moreover, indole ring inserts into interior of the pocket where benzyl group of MC1420 located, and forms aromatic interaction with Trp84 (Figs. 5E and 5F). However, **6** cannot interact with residues e.g. Tyr70 and Trp279, which make  $\pi$ - $\pi$  interactions with the right part of MC1420. And interacting with this residue may contribute to binding affinity.

Both lobeline and MC1420 are chemically different from compound **6**, however resulted with similar binding modes in corresponding receptors. Moreover, we found the trimethylammonium group of **6** can target to hydrophobic pockets of both receptors and make hydrophobic/aromatic interactions, and this role is supported by stronger analgesic effects of **6** than **5**, which contains a dimethylamine group and resulted in weaker interactions with corresponding targets and lower binding affinity.

## Conclusion

Pain is a common clinical symptom and a major health problem plague the quality of life for many people. Available analgesics—opioids, NSAIDs, and amine reuptake inhibitors—have varying, but typically low levels of analgesic efficacy, and are generally coupled with deleterious effects. So nature-derived products and their semi-synthetic derivatives serve as better candidates. In this research, we used 5-benzyloxyindole as the raw material to design and synthesize bufotenine (**5**) and its quaternary ammonium salt (**6**), the total yields were 66.2% and 59.6%. One such outcome is compound **6**, a derivative of compound **5**, and their analgesic activities were evaluated on the behavior of formalin induced pain in mice. The analgesic evaluation showed that compound **5** and compound **6** had strong effects on the behavior of formalin induced pain in mice. Subsequent experiments also showed that compound **6** shows synergistic analgesia with morphine painful effect. In conclusion, compound **5** is an analgesic active molecule and play a vital role in the analgesic effect of VB and compound **6** exhibits outstanding analgesic activity in vivo. Taking into account the potential biotechnological and pharmacological, compound **6** can serve as a latent analgesic drug candidate molecule.

In order to further investigate the molecular mechanism of this analgesic effect, in silico target prediction were performed on 36 analgesic-related targets (including 15 G protein-coupled receptors, 6 enzymes, 13 ion channels, and 2 others) using reverse docking. Both docking scores and ligand binding free energy were utilized to evaluate these targets, and finally 2 target (acetyl cholinesterase (AChE) and  $\alpha$ 4 $\beta$ 2 nicotinic acetylcholine receptor (nAChR)) were determined and corresponding binding mode were presented. The phenolic hydroxyl group of compound **6** forms hydrogen bond interaction with Glu199. Binding mode indicates the trimethylammonium group of compound **6** are also located in the hydrophobic area. Moreover, indole ring inserts into interior of the pocket where benzyl group of MC1420 located, and forms aromatic interaction with Trp84. However, com-

ound **6** cannot interact with residues e.g. Tyr70 and Trp279, which make  $\pi$ - $\pi$  interactions with the right part of MC1420. And interacting with this residue may contribute to binding affinity. Therefore, we guessed that the trimethylammonium group of compound **6** which form hydrophobic interaction with corresponding hydrophobic sub-pocket, resulting in highly related to binding affinity and analgesic affect.

## Experimental

### Chemistry

All commercially purchased raw materials and solvents were chemical pure and used without further purification unless otherwise specified. The progress of reactions was monitored by TLC analysis carried out on 0.15–0.20 mm Yantai silica gel plates RSGF 254 (Qingdao Kangyexin, China; 300–400 meshes) using UV light as the visualizing agent. <sup>1</sup>H NMR and <sup>13</sup>C NMR spectra were recorded on Bruker 500 MHz spectrometer (Bruker Co., Germany), with samples diluted in deuterated chloroform or DMSO and achievement of 32 scans. Tetramethylsilane (TMS) was considered as the internal standard. Chemical shifts ( $\delta$  values) and coupling constants ( $J$  values) are given in ppm and Hz respectively. Abbreviations used are s (singlet), d (doublet), t (triplet), q (quartet), b (broad) and m (multiplet). ESI-MS spectra were recorded on a Waters Synapt HDMS spectrometer.

2-(5-(Benzyloxy)-1*H*-indol-3-yl)-2-oxoacetyl chloride (**8**). A mixture of 5-benzyloxyindole (**7**) (220 mg, 1.0 mmol) and oxalyl chloride (175  $\mu$ L, 2.0 mmol) was stirred in anhydrous diethyl ether for 30 min at room temperature, the red solid obtained was collected by filtration, repeated washed with ether, and dried under vacuum to produce compound **8** (290 mg), with the crude yield was 94%.

2-(5-(Benzyloxy)-1*H*-indol-3-yl)-*N,N*-dimethyl-2-oxoacetamide (**9**). A solution of NaOH (170 mg, 4.25 mmol) in water (4.15 ml) was added dropwise into the reaction mixture of compound **8** (310 mg, 1.0 mmol) with a small amount of anhydrous diethyl ether and dimethylamine hydrochloride (350 mg, 4.29 mmol) in 30 min at 25 °C, the solid appeared was filtered to the crude product of compound **9**. After drying, it was directly mixed with silica gel and separated by column chromatography, using ethyl acetate as the eluent and obtain the pure product of compound **10** (288.6 mg), as a white solid, with a yield of 90%. <sup>1</sup>H NMR (500 MHz, CDCl<sub>3</sub>)  $\delta$ : 8.95 (s, 1H), 7.99 (d,  $J$  = 2.1 Hz, 1H), 7.91 (d,  $J$  = 3.2 Hz, 1H), 7.52 (d,  $J$  = 7.4 Hz, 2H), 7.42 (t,  $J$  = 7.5 Hz, 2H), 7.35 (dd,  $J$  = 13.1, 8.1 Hz, 2H), 7.05 (dd,  $J$  = 8.8, 2.5 Hz, 1H), 5.18 (s, 2H), 3.11 (d,  $J$  = 12.4 Hz, 6H); ESI-MS  $m/z$  321 [M - H]<sup>-</sup>, 323 [M + H]<sup>+</sup>, 345 [M + Na]<sup>+</sup> (Fig. S1).

2-(5-Hydroxy-1*H*-indol-3-yl)-*N,N*-dimethyl-2-oxoacetamide (**10**). At room temperature, compound **9** (50 mg, 0.155 mmol) and 10% palladium on activated carbon (5.0 mg) was solvated in mixture solution (MeOH : THF = 1 : 2) and the reaction vessel was purged with N<sub>2</sub>, and then with H<sub>2</sub>, and the solution was allowed to stir vigorously under an atmosphere of H<sub>2</sub>. After 18 h, all starting material was consumed. The re-

action solution was then filtered through a bed of celite and washed with EtOAc and concentrated. Silica gel mixing for column chromatography separation, dichloromethane: methanol = 20 : 1 as the eluent, the pure compound **10** (33.5 mg) was obtained, is an oily substance and the yield was 92%. <sup>1</sup>H NMR (500 MHz, DMSO) δ: 12.07 (s, 1H), 9.17 (s, 1H), 7.96 (d, *J* = 3.2 Hz, 1H), 7.71–7.16 (m, 2H), 6.76 (dd, *J* = 8.7, 2.3 Hz, 1H), 6.07–5.54 (m, 1H), 2.98 (s, 3H), 2.91 (s, 3H); ESI-MS *m/z* 231[M – H]<sup>–</sup>, 233 [M + H]<sup>+</sup>, 255 [M + Na]<sup>+</sup> (Fig. S2).

3-[2-(Dimethylamino)ethyl]-1*H*-indol-5-ol (**5**). To form a well-stirred suspension of lithium aluminum, LiAlH<sub>4</sub> (20.1 mg, 0.9 mmol) was dissolved in THF at 0 °C. The suspension was slowly added into a solution of compound **10** (35, 0.15 mmol) in THF and then the mixture was refluxed for 4 h under N<sub>2</sub>, then the reaction mixture was cool down to 40 °C and stirred for 10 h. Following cooling in an external ice bath, and cautious addition of 2M aqueous NaOH to quench to reaction. The inorganic solid was removed by filtration and the filter cake was washed using additional diethyl ether. The filtrate and washes were combined and dried over anhydrous magnesium sulfate and the solvents were removed in vacuo, then the silica gel was sampled and separated by column chromatography, using dichloromethane: methanol = 10 : 1 as the eluent to obtain compound **5** of pure product, about 26.2 mg, is a yellow-brown oily substance with a yield of 85%. <sup>1</sup>H NMR (500 MHz, DMSO) δ: 10.49 (s, 1H), 8.60 (s, 1H), 7.12 (d, *J* = 8.6 Hz, 1H), 7.04 (d, *J* = 2.1 Hz, 1H), 6.81 (d, *J* = 2.2 Hz, 1H), 6.59 (dd, *J* = 8.6, 2.3 Hz, 1H), 2.79–2.72 (m, 2H), 2.61–2.54 (m, 2H), 2.29 (s, 6H) (Fig. S3); <sup>13</sup>C NMR (126 MHz, DMSO) δ: 150.54, 131.24, 128.35, 123.38, 112.08, 111.99, 111.60, 102.66, 60.45, 45.58, 23.67; ESI-MS *m/z* 203[M – H]<sup>–</sup>, 205 [M + H]<sup>+</sup>, 227 [M + Na]<sup>+</sup> (Fig. S3, S4).

2-(5-Hydroxy-1*H*-indol-3-yl)-*N,N,N*-trimethylethan-1-aminium (**6**). Under dark conditions, take compound **5** (50 mg, 0.25 mmol) dissolved in methanol, add methyl iodide (2.2 ml, 3.5 mmol), after the mixture was the reaction to 36 h. The filter cake obtained was collected by filtration, repeatedly washed with methanol. Then the filter cake is resolved in methanol, excess AgCl was added, and the reaction was continued under dark conditions. After filtering, the filter residue was taken, mixed with neutral alumina and separated by column chromatography, Dichloromethane: methanol = 5 : 1 as the eluent to obtain the pure product of compound **6** (55.1 mg), which is a purple-brown oil with a yield of 90%. <sup>1</sup>H NMR (500 MHz, DMSO) δ 10.71 (s, 1H), 8.72 (s, 1H), 7.15 (dd, *J* = 9.2, 5.2 Hz, 2H), 6.91 (d, *J* = 1.7 Hz, 1H), 6.66 (dd, *J* = 8.6, 2.0 Hz, 1H), 3.56–3.48 (m, 2H), 3.17 (s, 9H), 3.11–3.02 (m, 2H) (Fig. S5); <sup>13</sup>C NMR (126 MHz, DMSO) δ: 150.90, 131.21, 127.85, 124.24, 112.31, 112.14, 107.75, 102.67, 65.69, 52.61, 19.17; ESI-MS *m/z* 218 [M – H]<sup>–</sup>, 220 [M + H]<sup>+</sup>, 242 [M + Na]<sup>+</sup> (Fig. S5, S6).

#### Pharmacology

##### Chemicals and reagents

Compound **5** (purity ≥ 98%), compound **6** (purity ≥

98%) and morphine (purity ≥ 98%). All the other chemicals/reagents used for various assays were of research-grade and were purchased from Sigma Aldrich (USA), unless otherwise stated.

##### Animals maintenance and ethical prerequisites

All procedures involving animals were conducted in accordance with the ethical guidelines established by the International Association for the Study of Pain [19] and the protocols were approved by the Animal Committee of Nanjing University of Chinese Medicine (Approval number, ACU171001). Health SPF grade adult ICR mice, female, weighing 18–22 g, age 6–8 weeks were used for different experiments with provided by Nanjing QingLongShan, China. Before the experiment, all mice were kept adaptively in the animal room of standard laboratory for a week, the room temperature was maintained at 20–25 °C, the relative humidity was 40%–60%, The animals were housed in a room with a normal 12-h light-dark cycle during the experiment, and were fed with the standard pellet diet with water ad libitum.

##### Dose formulation for in vivo experimentation

The formalin test is a widely used model of pain and this model has been used in mice. 20 μL 2.5% formalin (0.925% formaldehyde) solution was used as a modeling solution according to Salinas-Abarca *et al.* [20]. In all experiments, compound **5** and compound **6** used two doses of 5, 15 mg·kg<sup>–1</sup>, and morphine hydrochloride (0.25 mg·kg<sup>–1</sup>) was used as a standard drug according to Benjamin *et al.* [21].

##### Formalin-induced paw licking test

All behavioral experiments were carried out with the investigators blind to treatment conditions. The test was also determined by following the formalin test as reported by Tran L *et al.* [22] and later modified by Zhang S *et al.* [23]. Select the mice with normal ICR were randomly divided into six different groups consisting ten to twelve mice in each group according to body weight. Then mice in each group were administered by intraperitoneal injection (i.p.) of 0.1 mL/10 g. 15 min after administration, about 20 μL of 2.5% formalin (0.925% formaldehyde) was injected into the right hind paw subcutaneously. This provokes a sequence of responses such as licking, biting and shrinking indicating nociceptive behavior. compound **5** (5, 15 mg·kg<sup>–1</sup>), compound **6** (5, 15 mg·kg<sup>–1</sup>) and morphine (0.25 mg·kg<sup>–1</sup>) were given 30 min before injection of formalin, and the mice were observed. The amount of time (in seconds) spent in licking and biting of the injected paw was quantified and recorded.

##### Collaborative analgesic test

Morphine is also a classical opioid analgesic, which has a strong analgesic effect. Taking this into consideration, we designed an experiment to evaluate the synergistic analgesic effect of morphine and compound **6** (5, 15 mg·kg<sup>–1</sup>). The test was carried out according to the method described by Shetty and Anika [24] and modified by Zhang HL *et al.* [25]. Using a plantar test (37 370, Ugo Basile Plantar Test Apparatus, Italy) and preselect the mice with pain response within 30 s. Place healthy SPF adult ICR mice in a hot plate instrument, set the

temperature at  $55 \pm 0.5$  °C, measure the PWTL of the mice twice, per 5 min, and withdrawing the hind paw of mice as the observation index. If the mice do not lick the hind paw within 30 s, escape or jump, they will be discarded and replaced. The time of the mice licking the first foot before administration was recorded as the PWTL. Pre-selected qualified mice were divided into normal saline group, morphine hydrochloride group, compound **6** (5, 15 mg·kg<sup>-1</sup>) groups, and morphine + compound **6** (0.25 ± 5, 15 mg·kg<sup>-1</sup>) groups, 12 mice in each group, then mice in each group were administered by intraperitoneal injection (i.p.) of 0.1 mL/10 g. Before drug intervention, adjust the temperature of the hot plate to 55 °C and keep for 60 min. At the point of 30, 60, 90, 120 min after administration, we measured three times per mice

$$\text{age prolongation of PWTL} = \frac{(\text{Pain threshold after administration} - \text{Pain threshold before administration})}{\text{Pain threshold before administration}} \times 100\%$$

### Computational methods

#### Target structures retrieval/preparation

GPCR crystal structures were retrieved from Protein Data Bank (<https://www.rcsb.org/>, last accession data, 1<sup>st</sup> of Jue. 2020). All protein PDB files were prepared within the Schrödinger. Maestro (version 11.5) was performed to split chains, separately extract the ligand, protein, and (if present) waters, ions, organometallics and cofactors, and subsequently protein-ligand complexes were prepared using the Protein Preparation Wizard in Maestro with default options [26]. The prepared protein-ligand complex were finally used to generated grid files using Receptor Grid Generation by picking the co-crystallized ligand to define the binding site. Two binding sites are investigated if there are two ligands which binding in different sites within one structure. All structures of corresponding receptors were investigated, and however, at most 6 structures (higher resolution would be preferred) were involved if more than 6 structures were released for one receptor.

#### Docking and rescoring calculations

Compound **6** was prepared from one-dimensional SMILES code with charge information to three-dimensional structures using Ligpre in Schrödinger. All docking was executed in Virtual Screening Workflow using Glide XP (extra precision) mode [27]. Enhanced sampling were used to generated multiple conformations, and also performed post-docking minimization. And for each ligand, 30 poses were generated. Subsequently, MMGBSA were calculated for all docking poses using Prime.

## Appendix A. Supporting information

All the supporting information of this paper can be requested by sending E-mails to the corresponding authors.

## References

[1] Ul Hoque MS, Chowdhury MS, Paul A, et al. *In vivo* analgesic effect of different extracts of *Hopea odorata* leaves in mice and *in silico* molecular docking and ADME/T property analysis of

and the PWTL was the average of it. If the mice have no pain reaction within 60 s, take it out immediately and calculate according to 60 s. Data was produced by comparing observed values with that values of the control group and morphine group.

#### Statistical analysis

All experimental data were analyzed and plotted using statistical analysis software SPSS 22.0 and GraphPad Prism 8.0. The data are presented as mean ± SEM, and comparison between groups was made with two-way ANOVA and Dunnett's *t*-test. The *P* values < 0.05 were considered statistically significant. Percentage prolongation of PWTL was calculated using the formula:

some isolated compounds from this plant [J]. *J Basic Clin Physiol Pharmacol*, 2018, **30**(1): 121-130.

[2] Woolf CJ. What is this thing called pain? [J]. *J Clin Invest*, 2010, **120**(11): 3742-3744.

[3] Ji RR, Xu ZZ, Gao YJ. Emerging targets in neuroinflammation-driven chronic pain [J]. *Nat Rev Drug Discov*, 2014, **13**(7): 533-548.

[4] Maatuf Y, Geron M, Priel A. The role of toxins in the pursuit for novel analgesics [J]. *Toxins (Basel)*, 2019, **11**(2): 131.

[5] McGettigan P, Henry D. Cardiovascular risk and inhibition of cyclooxygenase: a systematic review of the observational studies of selective and nonselective inhibitors of cyclooxygenase 2 [J]. *JAMA*, 2006, **296**(13): 1633-1644.

[6] Colloca L, Ludman T, Bouhassira D, et al. Neuropathic pain [J]. *Nat Rev Dis Primers*, 2017, **3**: 17002.

[7] Wei WL, Hou JJ, Wang X, et al. Venenum bufonis: An overview of its traditional use, natural product chemistry, pharmacology, pharmacokinetics and toxicology [J]. *J Ethnopharmacol*, 2019, **237**: 215-235.

[8] Yang Q, Zhou XX, Zhang M, et al. Angel of human health: current research updates in toad medicine [J]. *Am J Transl Res*, 2015, **7**(1): 1-14.

[9] Coates MD, Tekin I, Vrana KE, et al. Review article: the many potential roles of intestinal serotonin (5-hydroxytryptamine, 5-HT) signalling in inflammatory bowel disease [J]. *Aliment Pharmacol Ther*, 2017, **46**(6): 569-580.

[10] Yekkirala AS, Roberson DP, Bean BP, et al. Breaking barriers to novel analgesic drug development [J]. *Nat Rev Drug Discov*, 2017, **16**(8): 545-564.

[11] Lee A, Lee K, Kim D. Using reverse docking for target identification and its applications for drug discovery [J]. *Expert Opin Drug Discov*, 2016, **11**(7): 707-715.

[12] Chong CR, Sullivan DJ. New uses for old drugs [J]. *Nature*, 2007, **448**(7154): 645-646.

[13] Harvey AL, Edrada-Ebel R, Quinn RJ. The re-emergence of natural products for drug discovery in the genomics era [J]. *Nat Rev Drug Discov*, 2015, **14**(2): 111-129.

[14] Ahinko M, Niinivehmas S, Jokinen E, et al. Suitability of MMGBSA for the selection of correct ligand binding modes from docking results [J]. *Chem Biol Drug Des*, 2019, **93**(4): 522-538.

[15] Wang YY, Chen C. Synthesis of a deuterium-labelled standard of bufotenine (5-HO-DMT) [J]. *J Labelled Comp Radiopharm*, 2007, **50**(14): 1262-1265.

[16] Friesner RA, Murphy RB, Repasky MP, et al. Extra precision

- glide: docking and scoring incorporating a model of hydrophobic enclosure for protein-ligand complexes [J]. *J Med Chem*, 2006, **49**(21): 6177-6196.
- [17] Khorana N, Changwichit K, Ingkaninan K, *et al.* Prospective acetylcholinesterase inhibitory activity of indole and its analogs [J]. *Bioorg Med Chem Lett*, 2012, **22**(8): 2885-2888.
- [18] Queiroz MM, Queiroz EF, Zeraik ML, *et al.* Chemical composition of the bark of *Tetrapterys mucronata* and identification of acetylcholinesterase inhibitory constituents [J]. *J Nat Prod*, 2014, **77**(3): 650-656.
- [19] Eum S, Choi HD, Chang MJ, *et al.* Protective effects of vitamin E on chemotherapy-induced peripheral neuropathy: a meta-analysis of randomized controlled trials [J]. *Int J Vitam Nutr Res*, 2013, **83**(2): 101-111.
- [20] Salinas-Abarca AB, Avila-Rojas SH, Barragan-Iglesias P, *et al.* Formalin injection produces long-lasting hypersensitivity with characteristics of neuropathic pain [J]. *Eur J Pharmacol*, 2017, **797**: 83-93.
- [21] Ragen BJ, Maninger N, Mendoza SP, *et al.* The effects of morphine, naloxone, and kappa opioid manipulation on endocrine functioning and social behavior in monogamous titi monkeys (*Callicebus cupreus*) [J]. *Neuroscience*, 2015, **287**: 32-42.
- [22] Tran L, Greenwood-Van Meerveld B. Lateralized amygdala activation: importance in the regulation of anxiety and pain behavior [J]. *Physiol Behav*, 2012, **105**(2): 371-375.
- [23] Zhang S, Jin X, You Z, *et al.* Persistent nociception induces anxiety-like behavior in rodents: role of endogenous neuropeptide S [J]. *Pain*, 2014, **155**(8): 1504-1515.
- [24] Shetty S, Anika S. *Laboratory Manual of Pharmacology and Toxicology* [M]. Fourth Dimension Publishers, 1982.
- [25] Zhang HL, Han R, Chen ZX, *et al.* Analgesic effects of rezeptin, a chemically modified cobratoxin from Thailand cobra venom [J]. *Neurosci Bull*, 2006, **22**(5): 267-273.
- [26] Sastry GM, Adzhigirey M, Day T, *et al.* Protein and ligand preparation: parameters, protocols, and influence on virtual screening enrichments [J]. *J Comput Aided Mol Des*, 2013, **27**(3): 221-234.
- [27] Friesner RA, Banks JL, Murphy RB, *et al.* Glide: a new approach for rapid, accurate docking and scoring. 1. Method and assessment of docking accuracy [J]. *J Med Chem*, 2004, **47**(7): 1739-1749.

**Cite this article as:** ZHAO Chao, CHEN Min, SUN Shan-Liang, WANG Jiao-Jiao, ZHONG Yue, CHEN Huan-Huan, LI He-Min, XU Han, LI Nian-Guang, MA Hong-Yue, WANG Xiao-Long. Bufotenine and its derivatives: synthesis, analgesic effects identification and computational target prediction [J]. *Chin J Nat Med*, 2021, **19**(6): 454-463.